AGU PUBLICATIONS

Geophysical Research Letters

Supplemental Material for

Naphthalene-derived secondary organic aerosols interfacial photosensitizing properties

Xinke Wang[1], Rachel Gemayel[1], Vahe J. Baboomian[2], Kangwei Li[1], Antoinette Boreave[1], Clement Dubois[1], Sophie Tomaz[1], Sebastien Perrier[1], Sergey A. Nizkorodov[2], Christian George[1,*]

[1]Univ Lyon, Université Claude Bernard Lyon 1, CNRS, IRCELYON, F-69626, Villeurbanne, France.

[2]Department of Chemistry, University of California, Irvine, Irvine, California, 92697, USA.

[*]To whom correspondence should be addressed. Email: christian.george@ircelyon.univ-lyon1.fr

Contents of this file

Introduction

The following text, tables, and figures are referred to as supplementary material in the main text. Text sections S1-S3 provide detailed information on HRMS analysis of Nap-derived SOA, chemical characteristics of Nap-derived SOA, and SMPS and AMS measurements, respectively. Figures S1-S2 show the histograms of atom number in C- (black) and O- (red) containing compounds and the Van Krevelen diagram for CHO compounds detected in Nap-derived SOA samples. Table S1 lists all organic compounds in Nap-derived SOA, together with their *m/z*, peak abundances, RDBE, and elemental ratios.

Text S1. HRMS analysis of Nap-derived SOA

Nap-derived SOA was collected onto 47 mm quartz fiber filters (Tissuquartz 2500QAT, PALL Life Sciences) with a sampling time of 15 min at the flow rate of 4.05 L min^{-1}. The blank samples were collected using the same procedure but without injecting naphthalene. All filter samples were extracted with two subsequent 6 mL extractions of acetonitrile (Optima® LC/MS, Fischer Scientific, USA) and agitated for 20 min on an orbital shaker set at 1000 rpm. The combined extracts were filtered through a 0.2 μm polytetrafluoroethylene membrane (13 mm, Pall Corporation, USA) using a glass syringe. Next, 0.5 mL of the extracts were diluted by adding 0.5 mL of water (Optima® LC/MS, Fischer Scientific, USA), before being analyzed by an Orbitrap high resolution mass spectrometer (HRMS, Q Exactive, Thermo Scientific, Bremen, Germany) with heated electrospray ionization (HESI). The diluted extracts were injected in a direct-infusion mode using a Hamilton syringe at a flow rate of 5 μL min^{-1} and analyzed in negative (ESI-) mode. The details of the HRMS analysis has been described in previous studies (Wang et al., 2020; Wang et al., 2016).

In this study, Xcalibur software (V2.2, Thermo Scientific) was used to analyze the obtained mass spectra and export mass lists (Lin et al., 2012). All ions with a signal-to-noise ratio (s/n) ≥ 3, signal intensity : background ratio > 10, and in the m/z range of 50-750 were exported. Chemical formula (i.e., $[M-H]^-$ and $[M+H]^+$) assignments for these ions were calculated using a mass tolerance of ±3 ppm in ESI- and ±4 ppm in ESI+ modes, respectively (Lin et al., 2012). Additionally, formulas were further constrained by setting H/C and O/C in the ranges of 0.3-3 and 0-3, respectively.

Text S2. Chemical characteristics of Nap-derived SOA

A total of 97 organic compounds were determined in ESI-. All formulas, together with their m/z, intensities, ring and double bond equivalence (RDBE), and elemental ratios are listed in Table S1. Notably, ESI-HRMS is highly sensitive to polar compounds, while being quite insensitive to non-polar ones, as those exhibit very poor ionization efficiency (Kuang et al., 2018). Therefore, many non-polar compounds might not have been measured in this study. In addition, ESI techniques are prone to matrix effects and varying ionization efficiencies for different compounds, meaning the signal intensities reported here do not represent actual concentrations.

As shown in Figure S1, C_{10} compounds (i.e., compounds with ten carbon atoms) are the most dominant ones, accounting for 18.4% of total determined formulas and represent the ring-retaining products (Chan et al., 2009). Both the ring-opening products (i.e., C_7, C_8, and C_9 series) and the dimers (i.e., C_{18}, C_{19} and C_{20}) are also important products from the OH-initiated oxidation of naphthalene. In addition, more than 78% of determined organic compounds contained more than 3 oxygen atoms (Figure S1), suggesting that these compounds bear multiple oxidation functional groups. Moreover, Figure S2 shows that most of these compounds have high degrees of unsaturation and oxygenation, highlighting their aromatic and polycyclic aromatic structures.

Notably, excitation in natural waters typically involves the promotion of an electron from an n or π orbital (the bonding orbitals common in carbonyl and aromatic compounds) to a higher energy anti-bonding orbital (π*), suggesting that carbonyl-containing aromatic compounds are well-suited candidates to act as photosensitizers (Canonica et al., 1995; Osburn & Morris, 2003). Therefore, in addition to naphthoquinone, other carbonyl-containing aromatic products existing in Nap-derived SOA (Huang et al., 2019) probably also play an important role in the photosensitized oxidation of SO_2 and VOCs.

Text S3. SMPS and AMS descriptions

The SMPS instrument consists of a differential mobility analyzer (DMA, TSI 3081) and a condensation particle counter (CPC, TSI 3772, or TSI 3776). The gas flow was 0.3 L min^{-1} and the corresponding sheath flow was 3 L min^{-1}.

The ionization efficiency (IE) and relative ionization efficiency (RIE) of the AMS were calibrated using 300 nm ammonium nitrate particles. Ammonium nitrate (NH_4NO_3) particles were generated by a constant-output atomizer (TSI Model 3076), then dried by a silica dryer, size selected by a DMA, and then sent to the AMS and CPC simultaneously. Notably, the Nap-SOA used for the sulfate production measurement experiments were size selected at 100 nm diameter before being injected into the AFT. Therefore, dried monodispersed ammonium sulfate ($(NH_4)_2SO_4$) particles with the same size (i.e., 100 nm) were flowed into the AMS and SMPS simultaneously, and the collection efficiency (CE) of the AMS was derived by comparing the sulfate concentrations measured by the AMS and calculated by the SMPS. The particle size distributions of $(NH_4)_2SO_4$ measured by the SMPS were converted to mass concentrations using a density of 1.77 g cm^{-3} (Sarangi et al., 2016). The study of Allan et al. (2004) showed that the CE value depends on the RH of the sample air. As such, all experiments in our study had the aerosol flow RH prior to the analysis by AMS below 25%; therefore, the calculated CE is applicable for all experiments. The AMS analysis software Squirrel version 1.60P and Pika version 1.20P were used to analyze the obtained mass spectra.

Figures

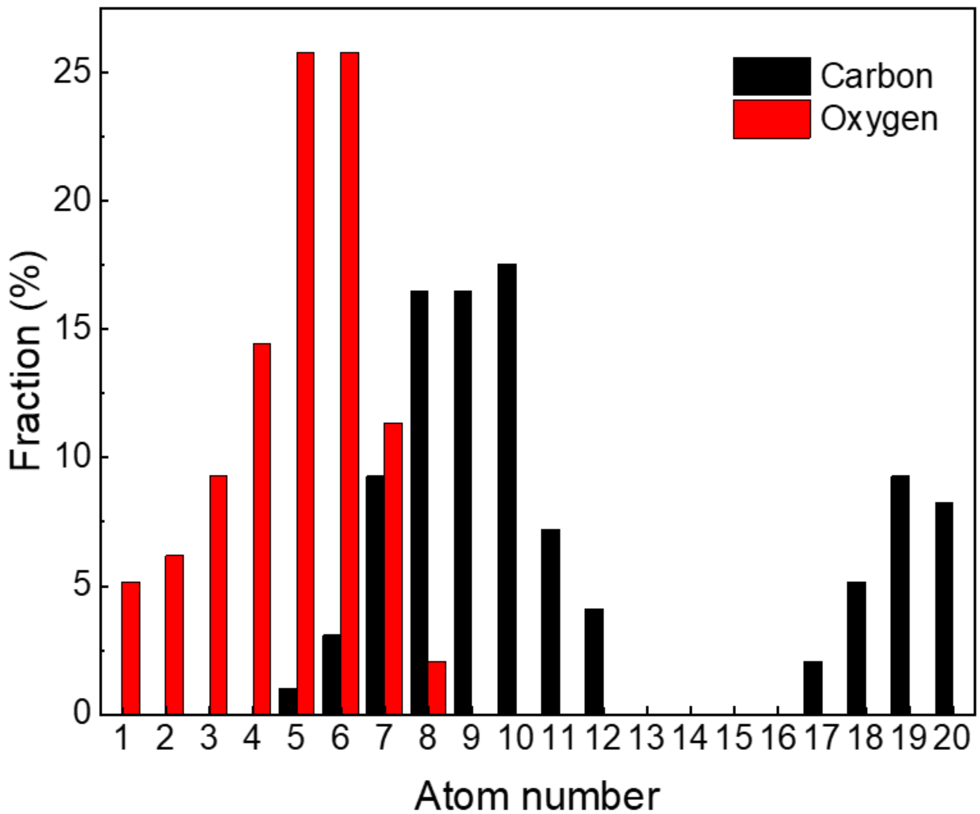

Figure S1. Histograms of atom number in C- (black) and O- (red) containing compounds of the determined constituents in Nap-derived SOA samples.

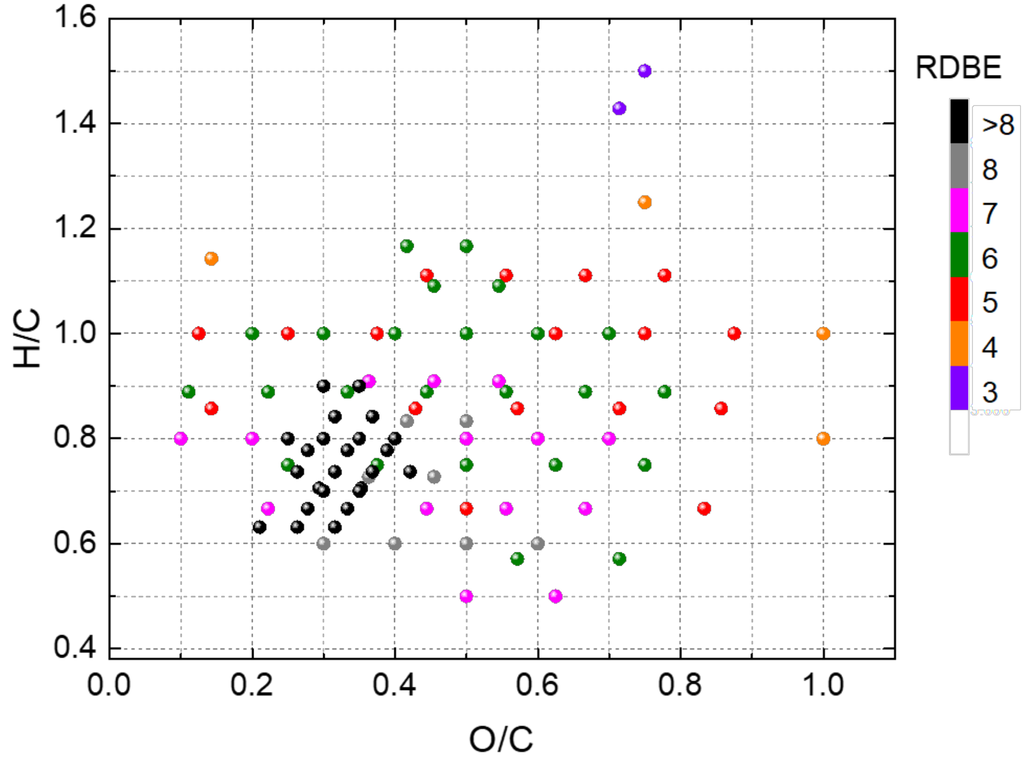

Figure S2. Van Krevelen diagrams for identified formulas in Nap-SOA. The color-coding indicates the RDBE values.

Table S1. All formulas, together with their *m/z*, intensities, ring and double bond equivalence (RDBE), and elemental ratios tentatively determined in Nap-derived SOAs.

m/z	assigned formula	Intensity	H/C	O/C	RDBE
105.0345	C_7H_6O	3.52×10^4	0.86	0.14	5
107.0501	C_7H_8O	1.35×10^3	1.14	0.14	4
119.0499	C_8H_8O	2.43×10^5	1.00	0.13	5
123.0087	$C_6H_4O_3$	1.13×10^4	0.67	0.50	5
131.0501	C_9H_8O	2.27×10^5	0.89	0.11	6
133.0294	$C_8H_6O_2$	3.92×10^5	0.75	0.25	6
135.0450	$C_8H_8O_2$	1.52×10^5	1.00	0.25	5
137.0242	$C_7H_6O_3$	5.95×10^5	0.86	0.43	5
142.9984	$C_5H_4O_5$	1.56×10^4	0.80	1.00	4
143.0500	$C_{10}H_8O$	1.15×10^5	0.80	0.10	7
145.0293	$C_9H_6O_2$	3.12×10^5	0.67	0.22	7
147.0450	$C_9H_8O_2$	7.93×10^5	0.89	0.22	6
149.0241	$C_8H_6O_3$	3.77×10^6	0.75	0.38	6
151.0034	$C_7H_4O_4$	8.24×10^3	0.57	0.57	6
151.0399	$C_8H_8O_3$	1.47×10^5	1.00	0.38	5
153.0191	$C_7H_6O_4$	1.59×10^5	0.86	0.57	5
154.9985	$C_6H_4O_5$	8.56×10^3	0.67	0.83	5
159.0449	$C_{10}H_8O_2$	1.60×10^5	0.80	0.20	7
161.0242	$C_9H_6O_3$	5.92×10^5	0.67	0.33	7
161.0606	$C_{10}H_{10}O_2$	2.17×10^3	1.00	0.20	6
163.0035	$C_8H_4O_4$	5.48×10^5	0.50	0.50	7
163.0399	$C_9H_8O_3$	2.05×10^6	0.89	0.33	6
165.0191	$C_8H_6O_4$	1.44×10^7	0.75	0.50	6
166.9983	$C_7H_4O_5$	9.55×10^3	0.57	0.71	6
167.0347	$C_8H_8O_4$	4.17×10^4	1.00	0.50	5
169.0140	$C_7H_6O_5$	3.55×10^4	0.86	0.71	5
173.0090	$C_6H_6O_6$	4.63×10^3	1.00	1.00	4
173.0241	$C_{10}H_6O_3$	9.04×10^5	0.60	0.30	8
173.0450	$C_7H_{10}O_5$	1.42×10^4	1.43	0.71	3
175.0398	$C_{10}H_8O_3$	5.12×10^6	0.80	0.30	7
177.0191	$C_9H_6O_4$	7.30×10^5	0.67	0.44	7
177.0553	$C_{10}H_{10}O_3$	2.10×10^5	1.00	0.30	6
178.9984	$C_8H_4O_5$	1.35×10^4	0.50	0.63	7
179.0347	$C_9H_8O_4$	2.00×10^6	0.89	0.44	6
181.0136	$C_8H_6O_5$	4.43×10^5	0.75	0.63	6
181.0504	$C_9H_{10}O_4$	3.33×10^4	1.11	0.44	5
183.0295	$C_8H_8O_5$	2.57×10^4	1.00	0.63	5
185.0089	$C_7H_6O_6$	1.08×10^4	0.86	0.86	5

189.0191	$C_{10}H_6O_4$	4.70×10^5	0.60	0.40	8
191.0347	$C_{10}H_8O_4$	2.48×10^6	0.80	0.40	7
193.0139	$C_9H_6O_5$	1.10×10^6	0.67	0.56	7
193.0501	$C_{10}H_{10}O_4$	7.06×10^5	1.00	0.40	6
195.0296	$C_9H_8O_5$	6.49×10^5	0.89	0.56	6
197.0088	$C_8H_6O_6$	2.84×10^4	0.75	0.75	6
197.0452	$C_9H_{10}O_5$	9.20×10^3	1.11	0.56	5
199.0245	$C_8H_8O_6$	2.03×10^4	1.00	0.75	5
201.0401	$C_8H_{10}O_6$	8.90×10^3	1.25	0.75	4
203.0346	$C_{11}H_8O_4$	2.89×10^4	0.73	0.36	8
203.0571	$C_8H_{12}O_6$	1.12×10^5	1.50	0.75	3
205.0139	$C_{10}H_6O_5$	9.57×10^4	0.60	0.50	8
205.0513	$C_{11}H_{10}O_4$	1.66×10^4	0.91	0.36	7
207.0295	$C_{10}H_8O_5$	1.41×10^6	0.80	0.50	7
209.0088	$C_9H_6O_6$	7.31×10^4	0.67	0.67	7
209.0450	$C_{10}H_{10}O_5$	6.48×10^5	1.00	0.50	6
211.0245	$C_9H_8O_6$	6.55×10^4	0.89	0.67	6
213.0401	$C_9H_{10}O_6$	5.14×10^3	1.11	0.67	5
215.0204	$C_8H_8O_7$	3.48×10^4	1.00	0.88	5
219.0295	$C_{11}H_8O_5$	1.35×10^4	0.73	0.45	8
221.0092	$C_{10}H_6O_6$	1.28×10^4	0.60	0.60	8
221.0454	$C_{11}H_{10}O_5$	4.10×10^4	0.91	0.45	7
223.0245	$C_{10}H_8O_6$	2.38×10^5	0.80	0.60	7
223.0608	$C_{11}H_{12}O_5$	4.49×10^4	1.09	0.45	6
225.0401	$C_{10}H_{10}O_6$	1.55×10^5	1.00	0.60	6
227.0193	$C_9H_8O_7$	6.79×10^3	0.89	0.78	6
229.0351	$C_9H_{10}O_7$	1.10×10^3	1.11	0.78	5
233.0451	$C_{12}H_{10}O_5$	9.71×10^3	0.83	0.42	8
237.0401	$C_{11}H_{10}O_6$	2.84×10^4	0.91	0.55	7
237.0766	$C_{12}H_{14}O_5$	2.23×10^4	1.17	0.42	6
239.0194	$C_{10}H_8O_7$	5.56×10^4	0.80	0.70	7
239.0563	$C_{11}H_{12}O_6$	3.23×10^4	1.09	0.55	6
241.0351	$C_{10}H_{10}O_7$	3.12×10^4	1.00	0.70	6
249.0401	$C_{12}H_{10}O_6$	7.66×10^3	0.83	0.50	8
253.0714	$C_{12}H_{14}O_6$	6.84×10^3	1.17	0.50	6
295.0606	$C_{17}H_{12}O_5$	6.92×10^3	0.71	0.29	12
303.0658	$C_{19}H_{12}O_4$	9.70×10^3	0.63	0.21	14
307.0608	$C_{18}H_{12}O_5$	8.97×10^3	0.67	0.28	13
309.0764	$C_{18}H_{14}O_5$	1.36×10^4	0.78	0.28	12
311.0557	$C_{17}H_{12}O_6$	5.84×10^3	0.71	0.35	12
319.0604	$C_{19}H_{12}O_5$	1.12×10^4	0.63	0.26	14
321.0762	$C_{19}H_{14}O_5$	7.23×10^3	0.74	0.26	13
323.0553	$C_{18}H_{12}O_6$	1.35×10^4	0.67	0.33	13

325.0710	$C_{18}H_{14}O_6$	2.41×10^4	0.78	0.33	12
335.0553	$C_{19}H_{12}O_6$	7.33×10^3	0.63	0.32	14
335.0938	$C_{20}H_{16}O_5$	2.09×10^4	0.80	0.25	13
337.0711	$C_{19}H_{14}O_6$	3.96×10^4	0.74	0.32	13
339.0869	$C_{19}H_{16}O_6$	1.63×10^4	0.84	0.32	12
341.0662	$C_{18}H_{14}O_7$	1.30×10^4	0.78	0.39	12
349.0712	$C_{20}H_{14}O_6$	7.60×10^3	0.70	0.30	14
351.0870	$C_{20}H_{16}O_6$	3.73×10^4	0.80	0.30	13
353.0662	$C_{19}H_{14}O_7$	2.63×10^4	0.74	0.37	13
353.1025	$C_{20}H_{18}O_6$	7.92×10^3	0.90	0.30	12
355.0820	$C_{19}H_{16}O_7$	1.04×10^4	0.84	0.37	12
365.0661	$C_{20}H_{14}O_7$	8.09×10^3	0.70	0.35	14
367.0818	$C_{20}H_{16}O_7$	4.32×10^4	0.80	0.35	13
369.0609	$C_{19}H_{14}O_8$	8.74×10^3	0.74	0.42	13
369.0974	$C_{20}H_{18}O_7$	1.53×10^4	0.90	0.35	12
383.0767	$C_{20}H_{16}O_8$	1.18×10^4	0.80	0.40	13

References

Allan, J. D., Bower, K. N., Coe, H., Boudries, H., Jayne, J. T., Canagaratna, M. R., et al. (2004). Submicron aerosol composition at Trinidad Head, California, during ITCT 2K2: Its relationship with gas phase volatile organic carbon and assessment of instrument performance. *Journal of Geophysical Research D: Atmospheres*, *109*(23), 1–16. https://doi.org/10.1029/2003JD004208

Canonica, S., Jans, U. R. S., Stemmler, K., & Hoigne, J. (1995). Transformation Kinetics of Phenols in Water: Photosensitization. *Environmental Science & Technology*, *29*(7), 1822–1831.

Chan, A. W. H., Kautzman, K. E., Chhabra, P. S., Surratt, J. D., Chan, M. N., Crounse, J. D., et al. (2009). Secondary organic aerosol formation from photooxidation of naphthalene and alkylnaphthalenes: Implications for oxidation of intermediate volatility organic compounds (IVOCs). *Atmospheric Chemistry and Physics*, *9*(9), 3049–3060. https://doi.org/10.5194/acp-9-3049-2009

Huang, G., Liu, Y., Shao, M., Li, Y., Chen, Q., Zheng, Y., et al. (2019). Potentially Important Contribution of Gas-Phase Oxidation of Naphthalene and Methylnaphthalene to Secondary Organic Aerosol during Haze Events in Beijing. *Environmental Science and Technology*, *53*(3), 1235–1244. https://doi.org/10.1021/acs.est.8b04523

Kuang, B. Y., Yeung, H. S., Lee, C. C., Griffith, S. M., & Yu, J. Z. (2018). Aromatic formulas in ambient PM2.5 samples from Hong Kong determined using FT-ICR ultrahigh-resolution mass spectrometry. *Analytical and Bioanalytical Chemistry*, *410*(24), 6289–6304. https://doi.org/10.1007/s00216-018-1239-8

Lin, P., Rincon, A. G., Kalberer, M., & Yu, J. Z. (2012). Elemental composition of HULIS in the Pearl River Delta Region, China: Results inferred from positive and negative electrospray high resolution mass spectrometric data. *Environmental Science and Technology*, *46*(14), 7454–7462. https://doi.org/10.1021/es300285d

Osburn, C. L., & Morris, D. P. (2003). Photochemistry of chromophoric dissolved organic matter in natural waters. In E. W. Helbling & H. Zagarese (Eds.), *UV Effects in Aquatic Organisms and Ecosystems* (Vol. 1, pp. 185–218). The Royal Society of Chemistry. https://doi.org/10.1039/9781847552266-00185

Sarangi, B., Aggarwal, S. G., Sinha, D., & Gupta, P. K. (2016). Aerosol effective density measurement using scanning mobility particle sizer and quartz crystal microbalance with the estimation of involved uncertainty. *Atmospheric Measurement Techniques*, *9*(3), 859–875. https://doi.org/10.5194/amt-9-859-2016

Wang, X., Hayeck, N., Brüggemann, M., Abis, L., Riva, M., Lu, Y., et al. (2020). Chemical Characteristics and Brown Carbon Chromophores of Atmospheric Organic Aerosols Over the Yangtze River Channel: A Cruise Campaign. *Journal of Geophysical Research: Atmospheres*, *125*(16), 1–13. https://doi.org/10.1029/2020JD032497

Wang, X. K., Rossignol, S., Ma, Y., Yao, L., Wang, M. Y., Chen, J. M., et al. (2016). Molecular characterization of atmospheric particulate organosulfates in three megacities at the middle and lower reaches of the Yangtze River. *Atmospheric Chemistry and Physics*, *16*(4), 2285–2298. https://doi.org/10.5194/acp-16-2285-2016